Analysis of Array Feed Combining Performance Using Recorded Data

V. Vilnrotter
Communications and Systems Research Section

B. Iijima
Tracking Systems and Applications Section

Array feed combining data recorded with the Mark III data acquisition terminal at DSS 13 are analyzed to determine combining gain. The performance of the current real-time combining algorithm and that of a more complex algorithm that uses all pairwise correlations among the feeds are evaluated and compared. The results are extrapolated to lower receiver temperatures to predict the performance of future array feed receivers operating at much colder effective temperatures. For the cases considered, the improvement due to the more complex algorithm appears to be insignificant, even with very low-temperature receivers.

I. Introduction

The Ka-band array feed compensation system [1,2] is currently undergoing tests and evaluation at DSS 13. A conceptual design of this system is presented in Fig. 1. The real-time array feed system is capable of recovering losses due to elevation-dependent and wind-induced antenna deformations as well as of providing pointing corrections to the antenna. The current real-time combining algorithm measures the signal correlations between the central feed and the six outer feeds, computes the combining weights, and combines the weighted signals from all seven channels in order to increase the signal-to-noise ratio (SNR). This combining algorithm is optimum for the case of uncorrelated channel noise, but suboptimum when significant interchannel noise correlations exist. It was found that the noise in different channels is indeed slightly correlated, presumably due to near-field effects. Therefore, it is important to determine the amount of improvement that could be gained by using a more complex combining algorithm that produces the optimal combining weights in the presence of correlated noise, particularly if very low-noise cooled channels are employed. It was decided that data collected with the Mark III very long baseline interferometry (VLBI) data acquisition terminal (DAT) at DSS 13 would be used to resolve this issue. The recorded data can be analyzed to extract all pairwise correlations and construct sequences of on-source and off-source covariance matrices during an entire track. Because this is a very time-consuming operation, typically only one-hour segments are analyzed. As will be shown below, these covariance matrices can be modified to extrapolate results to lower-temperature receivers. Venus tracks on two different days were analyzed: on DOY 004 1995 under rainy conditions and later on DOY 020 1995 under clear, dry skies.

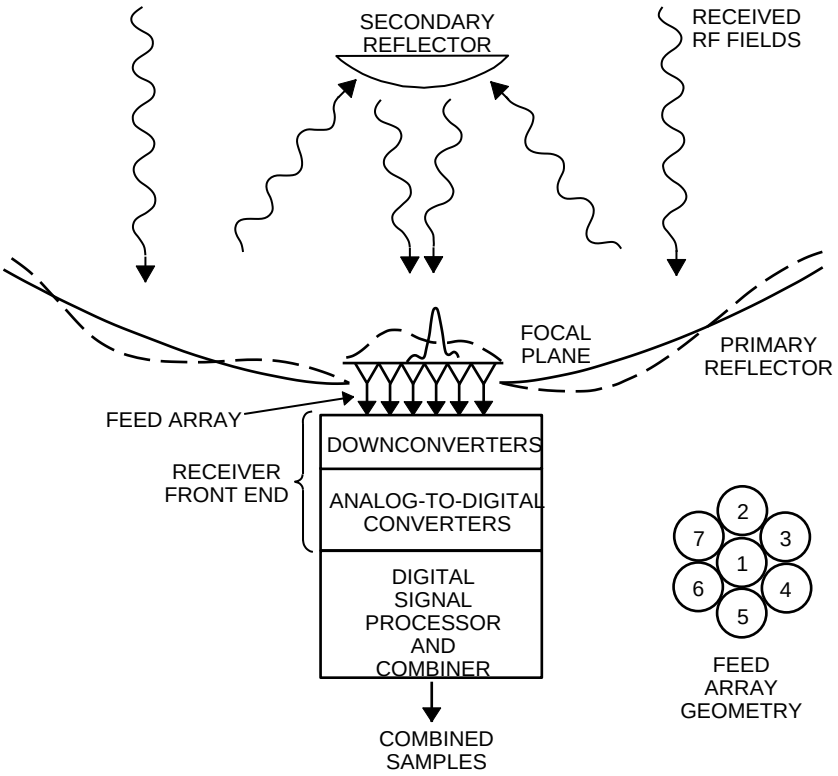

Fig. 1. Real-time antenna-compensation system conceptual design.

II. Representation of Received Samples

Although we specifically address the N-channel array feed compensation problem, the models and performance measures developed here apply equally well to any N-channel receiving system observing a common source in the presence of additive Gaussian noise. For a large class of such problems, the received samples in the kth channel can be represented as

$$r_k(i) = S_k a(i) + n_k(i) \tag{1}$$

where S_k is a complex number representing the magnitude and phase of the signal in the kth channel, $a(i)$ accounts for the time variation of the signal, and $n(i)$ are samples of additive Gaussian noise. The time function $a(i)$ represents modulation due to a variety of sources, including natural radiation from thermal sources and structured man-made signals. For thermal sources, $a(i)$ often can be modeled as a stationary random process with second-order statistics $E[a(I)] = 0$ and $E[|a(i)|^2] = 1$. When signals from a spacecraft are received, $a(i)$ takes on the structure of the modulation; for example, deep-space NASA telemetry employs residual-carrier modulation with square-wave subcarriers for the data, which typically are binary symbols. Thus, for NASA modulation, $a(i)$ might take the form

$$a(i) = \cos(\delta) + j\ s(i)\sin(\delta) \tag{2}$$

where δ is the modulation index and $s(i)$ is defined, according to the type of modulation, either as a pure data sequence, $d(i) = \pm 1$ or as a square-wave subcarrier-modulated data sequence [3].

III. Covariance of Received Samples

An N-channel array receiver observes the signal in the presence of additive noise. The additive noise is considered to be samples of a zero-mean complex Gaussian random process, $n_k(i)$, with statistics

$$\left.\begin{aligned} E\left[n_k(i)\right] &= 0 \\ E\left[|n_k(i)|^2\right] &= \sigma_k^2 \\ E\left[n_k(i)n_l^*(i)\right] &= \sigma_k\sigma_l\rho_{kl} \end{aligned}\right\} \tag{3}$$

Thus, different noise samples in each channel are independent, but corresponding samples in different channels are correlated. The noise statistics can be described completely by means of the noise-covariance matrix R, defined as

$$R = E\left[\underline{n}(i)\underline{n}^{\dagger}(i)\right] = \begin{bmatrix} \sigma_1^2 & & & \\ & \sigma_2^2 & & (\sigma_k\sigma_l\rho_{kl}) \\ (\sigma_l\sigma_k\rho_{lk}) & & \cdots & \\ & & & \sigma_N^2 \end{bmatrix} \tag{4}$$

where † means "conjugate transpose." The noise vector $\underline{n(i)}$ describes the time-aligned noise samples in all N channels, represented as

$$\underline{n(i)} = \begin{bmatrix} n_1(i) \\ n_2(i) \\ \cdot \\ \cdot \\ \cdot \\ n_N(i) \end{bmatrix} \tag{5}$$

The signal and weight vectors are defined as $\underline{S}^T = (S_1, S_2, \cdots, S_N)$ and $\underline{w}^T = (w_1, w_2, \cdots, w_N)$. Thus, with $\underline{r}(i) = a(i)\underline{S} + \underline{n}(i)$, the weighted combined samples can be represented as

$$z(i) = \sum_{k=1}^{N} w_k r_k(i) = \underline{w}^T\underline{r}(i) = \underline{r}(i)^T\underline{w} \tag{6}$$

Recalling the $E|a(i)|^2 = 1$, for independent signal and noise, the covariance of the received samples becomes

$$C = E\left[\underline{r}(i)\underline{r}^{\dagger}(i)\right] = \begin{bmatrix} |S_1|^2 + \sigma_1^2 & & & \\ & |S_2|^2 + \sigma_2^2 & & (S_kS_l^* + \sigma_k\sigma_l\rho_{kl}) \\ (S_lS_k^* + \sigma_l\sigma_k\rho_{lk}) & & \cdots & \\ & & & |S_N|^2 + \sigma_N^2 \end{bmatrix} \tag{7}$$

which can be expressed in compact form as $C = S\ S^{\dagger} + R$. The special case of equal noise power in every channel is of particular interest. Letting this case be denoted by C_0, we have

$$C_0 = \sigma^2 \begin{bmatrix} 1+SNR_1 & & \\ & 1+SNR_2 & \left(\frac{S_k S_l^*}{\sigma^2}+\rho_{kl}\right) \\ \left(\frac{S_l S_k^*}{\sigma^2}+\rho_{lk}\right) & \cdots & \\ & & 1+SNR_N \end{bmatrix} \tag{8}$$

where the SNR in the kth channel is $SNR_k = |S_k|^2/\sigma^2$, and σ^2 is the common noise power. This form of the covariance matrix will be used in Section VI for evaluating data recorded on the Mark III DAT. The correlator, which uses a 2-MHz bandwidth, produces correlation coefficients every 2 s, and the covariance matrices are estimates based on roughly ten 2-s averages obtained from the recorded data. As shown in the Appendix, the rms estimation error in the correlation coefficients due to additive noise is roughly 1.2×10^{-4}, which is on the order of a percent of the correlation coefficient for clear-weather data.

IV. Signal-to-Noise Ratio of Weighted Samples

SNR is an important indicator of performance in detection and estimation problems. The SNR of a weighted sum of samples, as defined in Eq. (6), can be expressed as the ratio of weighted signal and noise powers:

$$\begin{aligned} SNR &= \frac{power\ of\ weighted\ signal}{power\ of\ weighted\ noise} \\ &= \frac{E\left[|\underline{w^T}\ \underline{S}\ a(i)|^2\right]}{E\left[|\underline{w^T}\ \underline{n}(i)|^2\right]} \\ &= \frac{E\left[(\underline{w^T}\ \underline{S}\ a(i))(a(i)\ \underline{S^T}\ \underline{w})^*\right]}{E\left[(\underline{w^T}\ \underline{n}(i))\ (\underline{n^T}(i)\ \underline{w})^*\right]} \\ &= \frac{\underline{w^T}\ \underline{S}\ E\left[|a(i)|^2\right]\underline{S^\dagger}\ \underline{w^*}}{\underline{w^T} E\left[\underline{n}(i)\underline{n^\dagger}(i)\right]\underline{w^*}} \\ &= \frac{\underline{w^T}\ \underline{S}\ \underline{S^\dagger}\ \underline{w^*}}{\underline{w^T}\ R\ \underline{w^*}} \end{aligned} \tag{9}$$

The last equality shows the dependence of SNR on the signal vector, the weight vector, and the noise covariance matrix R. We can also write SNR in terms of the sample covariance, C, by noting that

$$1 + SNR = \frac{\underline{w^T}\ C\ \underline{w^*}}{\underline{w^T}\ R\ \underline{w^*}} \tag{10}$$

The right-hand side of Eq. (10) may be interpreted as the ratio of on-source to off-source samples; hence, it serves as a link between theory and experimental results.

V. Optimum Weights to Maximize SNR

The weight vectors can be used to achieve different results, including selection of a particular channel (or channels), suppression of unwanted channels, or maximization of combined SNR. As shown in [4–6],

the optimum weight vector for maximizing the SNR of a weighted sum in the presence of correlated noise is given by

$$\underline{w_0} = \alpha \left(R^{-1} \underline{S} \right)^* \tag{11}$$

where α is an arbitrary complex constant. Substitution of this weight vector into Eq. (9) yields the maximum SNR, SNR_{max}:

$$\begin{aligned} SNR_{max} &= \frac{(R^{-1}\underline{S})^\dagger \underline{S} \; \underline{S}^\dagger (R^{-1}\underline{S})}{(R^{-1}\underline{S})^\dagger \; R \; (R^{-1}\underline{S})} \\ &= \frac{(\underline{S}^\dagger R^{-1} \underline{S})(\underline{S}^\dagger R^{-1} \underline{S})}{\underline{S}^\dagger (R^{-1} R) R^{-1} \underline{S}} \\ &= \underline{S}^\dagger \; R^{-1} \; \underline{S} \end{aligned} \tag{12}$$

The maximum SNR of the combined channels is, therefore, a quadratic form of the complex signal vectors and the inverse of the noise covariance matrix.

VI. Extrapolating Results to Lower-Temperature Receivers

The array feed receiver under evaluation at DSS 13 has a system temperature close to 90 K due to the older style of high electron-mobility transistor (HEMT) amplifiers it employs in its front end (the T_{rec} recently measured for the central channel from the horns to the IF output was 86 K). It is difficult to demonstrate noise-cancellation concepts with a receiver operating at such a high temperature, although combining, which is a much larger effect, is easily demonstrated. It is of interest to determine how much SNR improvement could be expected from an operational array feed receiver that operated at a much lower receiver temperature, say in the neighborhood of $T_{rec} = 10$ K (believed to be achievable in the near future). Since the covariance matrix contains all of the necessary information, performance can be extrapolated to lower temperatures by properly scaling the covariance matrices obtained at the higher operating temperatures.

Let the total noise in the received samples, $n_k(i)$, be decomposed into independent and correlated components, $m_k(i)$ and $p_k(i)$:

$$n_k(i) = m_k(i) + p_k(i) \tag{13}$$

where $m_k(i)$ may be due to receiver noise and, hence, is independent between channels, while $p_k(i)$ may be caused by near-field effects, which introduce correlations among the channels. The noise power in these components is proportional to the receiver temperature, T_{rec}, and the sky temperature, T_{sky}, each measured at the station using a total power radiometer (TPR). While distinct samples in each channel are assumed to be independent, correlations between channels can be expressed as

$$E\left(n_k(i) n_l^*(i)\right) = E\left(m_k(i) m_l^*(i)\right) + E\left(p_k(i) p_l^*(i)\right) \tag{14}$$

where

$$E\left(p_k p_l^*\right) = \sigma_{n_k}\sigma_{n_l}\rho_{kl}, \quad k \neq l \tag{15}$$

and

$$E\left(m_k m_l^*\right) = \sigma_{m_k}\sigma_{m_l}\delta_{kl} \tag{16}$$

Although in general the total noise power in different channels may not be the same, an attempt has been made to equalize them at the station; hence, we shall consider the total noise powers equal in every channel.

The real-time equipment at the station cannot estimate all pairwise correlations. However, when the data are recorded on tape using the Mark III DAT and processed by the Block II correlator, all pairwise correlations can be extracted. The fundamental observables in this case are the on-source and off-source correlations while tracking a source such as Venus. The processed output of the Block II correlator consists of matrices of correlation coefficients, with the diagonal elements set equal to one; this is because the version of the correlator used to obtain the data is not able to make direct power measurements on individual channels, but can obtain accurate correlation coefficients. The difference of the on-source and off-source covariance matrices is used to estimate the signal outer product.

The matrix of correlation-coefficient estimates produced by the Block II correlator has the form [see Eq. (4)]

$$\frac{R}{\sigma^2} = \begin{bmatrix} 1 & & \\ & 1 & \dfrac{E\left(p_k p_l^*\right)}{\sigma^2} \\ \dfrac{E\left(p_l p_k^*\right)}{\sigma^2} & \cdots & \\ & & 1 \end{bmatrix} \tag{17}$$

Examples of the normalized off-source covariance matrix, along with the corresponding signal vector outer product, are shown in Figs. 2(a) and 2(b). These data were obtained on DOY 020 1995 while tracking Venus. Each entry is a complex number, with the real part on top and the imaginary part directly below it. Note that some correlation magnitudes are as large as 2 percent. The integration time for each data point is about 20 s, with a system bandwidth of 2 MHz. A large number of on-source and off-source covariance matrix estimates are produced during a typical track.

The first step in extrapolating to lower receiver temperatures is to multiply the normalized covariance matrix by our best estimate of the total noise power, obtained from a separate measurement (station TPR). The result of this operation is a correlation matrix with channel noise powers along the diagonal and correlation values as the off-diagonal elements:

$$R = \begin{bmatrix} \sigma^2 & & \\ & \sigma^2 & E\left(p_k p_l^*\right) \\ E\left(p_l p_k^*\right) & & \cdots \\ & & \sigma^2 \end{bmatrix} \tag{18}$$

For our purposes, the most important property of this matrix is that the off-diagonal elements do not depend on the receiver temperature, since they are due entirely to near-field effects; only the diagonal components depend on receiver temperature. Therefore, the second step in the extrapolation process is to replace the diagonal elements with those corresponding to the desired "cold" receiver; of course,

(a)

1.000000	–.007542	.001035	–.006829	.007624	.005999	–.000731
.000000	.007100	.013813	–.000901	–.007562	.000847	–.011098
–.007542	1.000000	–.007507	.000061	–.007053	–.004996	.004607
–.007100	.000000	.000639	.001059	.000532	–.000312	.020300
.001035	–.007507	1.000000	.002327	.002025	.011209	–.004210
–.013813	–.000639	.000000	–.000819	–.003251	–.000862	–.000254
–.006829	.000061	.002327	1.000000	.002253	–.000879	.001037
.000901	–.001059	.000819	.000000	.002477	.002951	.006362
.007624	–.007053	.002025	.002253	1.000000	.002155	.009739
.007562	–.000532	.003251	–.002477	.000000	–.000258	–.002947
.005999	–.004996	.011209	–.000879	.002155	1.000000	–.004928
–.000847	.000312	.000862	.002951	.000258	.000000	–.002911
–.000731	.004607	–.004210	.001037	.009739	–.004928	1.000000
.011098	–.020300	.000254	–.006362	.002947	.002911	.000000

(b)

.124654	.007412	.022224	.002046	–.004353	.017232	–.003007
.000000	.004831	–.019255	.020427	.013798	–.008207	–.002390
.007412	.000579	.000407	.000946	.000644	.001094	–.001330
–.004831	.000000	–.002051	.000359	.000938	–.001108	–.000831
.022224	.000407	.006819	–.002443	–.002304	.003591	.000520
.019255	.002051	.000000	.003038	.002134	.002232	–.000730
.002046	.000946	–.002443	.003528	.002552	–.001121	–.000281
–.020427	–.000359	–.003038	.000000	.001020	–.002674	.000514
–.004353	.000644	–.002304	.002552	.001587	–.001786	.000128
–.013798	–.000938	–.002134	–.001020	.000000	–.001805	–.000076
.017232	.001094	.003591	–.001121	–.001786	.003268	–.001175
.008207	.001108	–.002232	.002674	.001805	.000000	–.001061
–.003007	–.001330	.000520	–.000281	.000128	–.001175	.000114
.002390	.000831	.000730	–.000514	.000076	.001061	.000000

Fig. 2. Sample matrices used to evaluate performance: (a) normalized covariance matrix, off source, Venus DOY 020 1995 and (b) normalized signal vector outer product, Venus DOY 020 1995.

the contribution of near-field effects still has to be incorporated into the total noise power (diagonal elements). The extrapolated correlation matrix has the form

$$R_{cold} = \begin{bmatrix} \sigma_c^2 & & & \\ & \sigma_c^2 & E\left(p_k p_l^*\right) & \\ E\left(p_l p_k^*\right) & & \cdots & \\ & & & \sigma_c^2 \end{bmatrix} \tag{19}$$

where σ_c^2 denotes the noise power in a cold receiver. Once in this form, the correlation matrix can be used to predict the performance of future cold receivers, based on our current measurements.

VII. Numerical Results

In order to compare the performance of the array feed receiver with a more conventional single-horn receiver, it is useful to model the single horn as an equivalent array with fixed weights. Such a model is

reasonable since a single horn cannot change its response to accommodate changes in the field distribution. For example, we could model a single large horn as an array of seven smaller horns with equivalent total aperture area, as shown in Fig. 3. The weights of the outer horns, w_{hi}, can be adjusted to match the response of the larger horn. Once an equivalent weight vector is defined, similar operations can be applied to the data to characterize the performance of both the array feed and the conventional horn. Based on calculated horn radiation patterns, the weights of the outer horns were set to 0.05, while the weight of the central horn was set equal to 1.

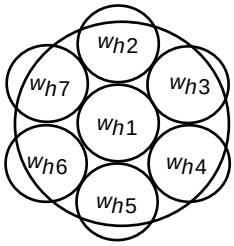

Fig. 3. Large horn and equivalent array.

A segment of Venus data recorded on DOY 020 1995 has been analyzed with the Block II correlator, and both on-source and off-source covariance matrices were generated roughly every 100–200 s over a 2500-s tracking interval. The recorded data have been analyzed in several different ways in order to evaluate array feed receiver performance in two different modes of operation, and also to compare its performance with that of a modeled single-horn receiver. The performance metric in all cases is output SNR. Results of the analysis are shown in Figs. 4(a) and 4(b).

Since the real-time algorithm computes the combining weights based only on the estimated signal correlation between the central and outer horns, these results were also calculated from the tapes and displayed in Fig. 4 as the points labeled "array feed (signal only)." In all cases, the actual SNR defined in Eq. (9) has been used; hence, these results incorporate the effects of imperfect weight estimates on the computed SNR. The maximum achievable SNR defined in Eq. (12) assumes perfectly known weights; hence, it cannot be achieved in practice. The points labeled "array feed (signal and noise covariance matrix)" represent the performance of a system that employs weights estimated from the entire noise covariance matrix, making full use of the available information to maximize SNR. However, even these weights suffer misadjustment noise due to limitations imposed by finite system bandwidth and observation time. The SNR of the array's central feed is also shown, along with the estimated performance of a modeled large horn.

Figure 4(a) represents the analysis of the actual data, assuming a receiver temperature of 90 K, while Fig. 4(b) shows the same results extrapolated to a 10-K receiver temperature. The average measured sky temperature during this track was about 30 K; hence, the actual total system temperature is 120 K, while the extrapolated cold system temperature is 40 K (the sum of the 10-K receiver temperature and the 30-K sky temperature). Since the received signal remains the same in both cases, it follows that the SNR of the cold receiver should be three times as great as that of the actual receiver; this is indeed true, and can be verified by direct comparison of Figs. 4(a) and 4(b). Because Venus is setting during this track, the elevation of the source changes from 21 to 14 deg, leading to degraded SNR due to increased signal loss and greater sky temperature at the lower elevations. Thus, the SNR of the central channel changes from 0.132 to 0.1, a loss of 1.2 dB. Since the array feed receiver recovers that part of the signal loss due to antenna distortions, the combined channel SNR always exceeds that of the central channel. At a 21-deg elevation, the combining gain is about 0.4 dB; at intermediate elevations, it is about 0.7 dB; and it approaches 0.8 dB at 14 deg, as shown in Fig. 4(a), but there is virtually no difference between the performance of the suboptimum weights (using signal only) and the optimum weights that employ all

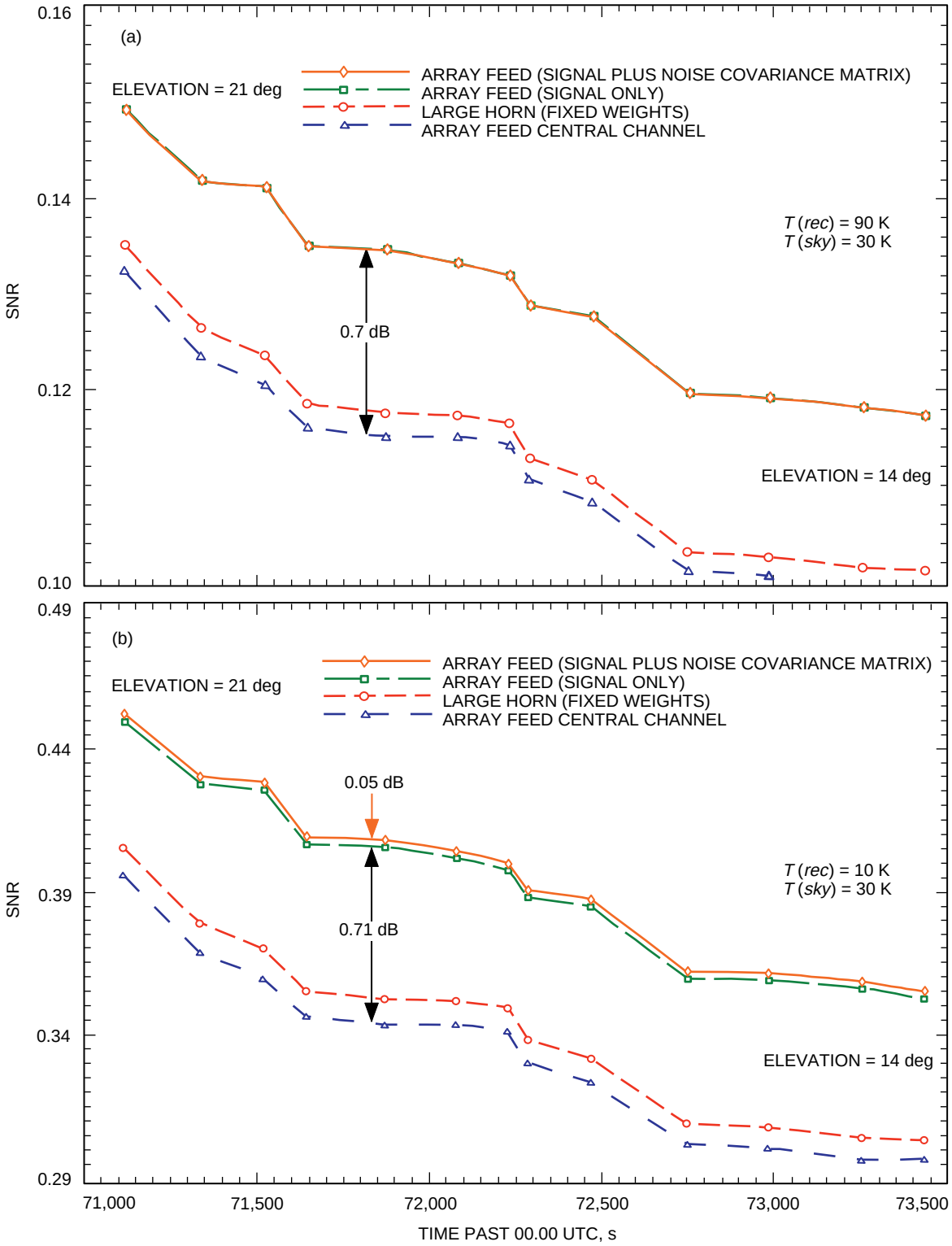

Fig. 4. Array feed combiner performance (Venus DOY 020 1995, clear and dry) for (a) a 90-K receiver and (b) a 10-K receiver.

pairwise correlations. Here gain is defined as the ratio of SNRs in dB, which is the improvement a ground receiver would observe while monitoring transmissions from a spacecraft. The gain with respect to the modeled large horn is somewhat less because, at all elevations, that horn collects more signal energy than the central horn of the array feed.

For the case of the cold receiver, the extrapolated curves of Fig. 4(b) show roughly 0.05 dB of additional combining gain when using the optimum weights. This improvement results from properly taking into account the complex correlation between all pairs of feeds. Much less improvement was found in rainy weather, as shown in Fig. 5; a similar analysis carried out for data recorded on DOY 004 1995, again using Venus as the source, shows no improvement when using the optimum weights. The physical mechanisms causing this surprising result are not well understood at this time; apparently, the increase in sky temperature was not accompanied by a corresponding increase in correlation, leading to reduced noise correlation coefficients. Efforts currently are under way to understand better the dependence of noise correlation on weather conditions.

The rainy-weather data of DOY 004 are much more erratic than the clear-weather data, due to the large changes in humidity along the line of sight (time-varying cloud thickness and occasional rain). Although there is no additional combining gain due to the use of optimum weights, the combining gain over the central channel is still significant, despite the increased signal loss due to the weather: at a 28-deg elevation, the gain is about 0.3 dB, while at 16 deg, it approaches 0.7 dB (the slight degradation over clear-weather gain is probably due to degraded weight estimates resulting from increased receiver noise). This result is not surprising since atmospheric attenuation reduces the total received signal power but does not alter the signal distribution over the array. Thus, array feed combining provides virtually weather-independent gain in telemetry SNR, which can always be used to advantage during reception.

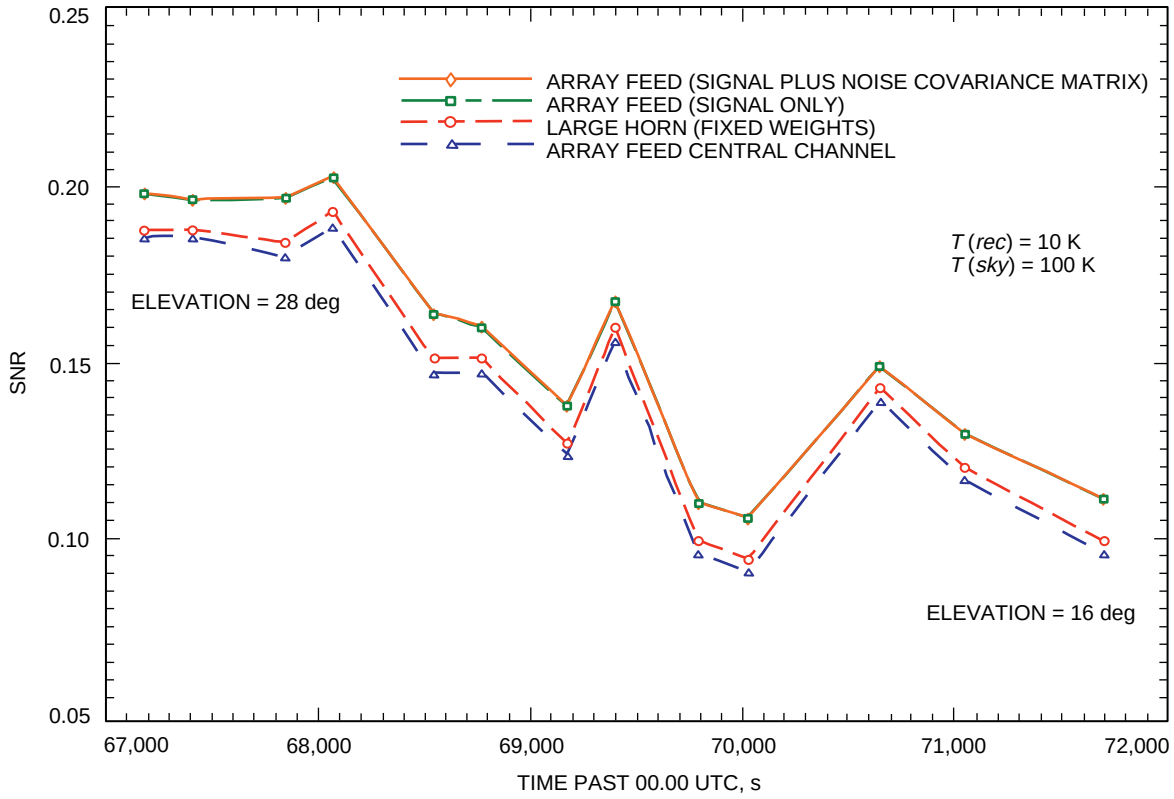

Fig. 5. Array feed combiner performance (Venus DOY 004 1995, light rain) for a 10-K receiver.

VIII. Summary and Conclusions

Array feed combining data recorded with the Mark III DAT at DSS 13 have been analyzed. The analysis was based on covariance matrices generated from the data, using all pairwise correlations between the feeds. With the current equipment, this information cannot be obtained at the station in real time, due to computational limits. Formulas were developed for estimating SNR, using on-source and off-source covariance matrices, and for modifying the measured covariance matrices to represent those of future cold receivers. Combining gain over the array feed central channel was obtained, along with the expected gain over a modeled large horn. Two different combining gains were defined: The first uses six simultaneous real-time correlation measurements between the central feed and the outer horns to compute the combining weights, while the second method employs all pairwise correlations (obtained by postprocessing taped data). The first method is optimum only when observing uncorrelated noise, while the second is also optimum in the presence of correlated noise. Analysis of the taped data indicates that, for the 90-K array feed receiver currently at DSS 13, noise correlation coefficients never exceed 2 percent; hence, the performances of the two algorithms are virtually identical. When extrapolating to cold receivers, the performance-limiting factor seems to be the sky temperature plus the temperature of antenna components outside of the receiver; thus, even if the receiver temperature were to reach absolute zero, the system temperature would still be near 30 K, due to external sources. Extrapolated results indicate that about 0.05 dB of additional combining gain could be obtained under clear, dry conditions, but that gain virtually disappeared in light rain. Data-gathering activities are continuing to determine if there are conditions under which greater noise correlations exist and to gain better understanding of the underlying mechanisms. In the meantime, it is clear that the real-time algorithm currently used by the array feed receiver is well suited to the task of determining and evaluating combiner performance.

References

[1] V. Vilnrotter, E. Rodemich, and S. Dolinar, "Real-Time Combining of Residual Carrier Array Signals Using ML Weight Estimates," *IEEE Trans. Comm.*, vol. 40, no. 3, pp. 604–615, March 1992.

[2] B. Iijima, D. Fort, and V. Vilnrotter, "Correlator Data Analysis for the Array Feed Compensation System," *The Telecommunications and Data Acquisition Progress Report 42-117, January–March 1994*, Jet Propulsion Laboratory, Pasadena, California, pp. 110–118, May 15, 1994.

[3] J. H. Yuen, *Deep Space Telecommunications Systems Engineering*, JPL Publication 82-76, Jet Propulsion Laboratory, Pasadena, California, July 1982.

[4] L. E. Brennan and L. S. Reed, "Theory of Adaptive Radar," *Array Processing Applications to Radar*, edited by S. Haykin, Stroudsburg, Pennsylvania: Dowden, Hutchinson and Ross, Inc., 1980.

[5] H. H. Tan, R. Liang, and P.-H. Suen, "Optimum Combining of Residual Carrier Array Signals in Correlated Noise," *The Telecommunications and Data Acquisition Progress Report 42-124, October–December 1995*, Jet Propulsion Laboratory, Pasadena, California, pp. 33–52, February 15, 1996.
http://tda.jpl.nasa.gov/tda/progress_report/42-124/124K.pdf

[6] K.-M. Cheung and V. Vilnrotter, "Channel Capacity of an Array System for Gaussian Channels With Applications to Combining and Noise Cancellation," *The Telecommunications and Data Acquisition Progress Report 42-124, October–December 1995*, Jet Propulsion Laboratory, Pasadena, California, pp. 53–62, February 15, 1996.
http://tda.jpl.nasa.gov/tda/progress_report/42-124/124D.pdf

[7] J. H. Van Vleck and D. Middleton, "The Spectrum of Clipped Noise," *Proc. IEEE*, vol. 54, no. 1, pp. 2–19, 1966.

Appendix

Extraction of Correlation Coefficients From Mark III VLBI Data Acquisition Terminal Data

The Mark III VLBI data acquisition terminal (DAT) was used to record the array feed signals. For each feed, the DAT single bit samples a 2-MHz passband at the Nyquist rate of 4×10^6 samples/s. Here we explain how the single-bit samples are used to compute correlation coefficients and to derive the uncertainties on those coefficients.

If the signals are stationary white noise processes with zero mean, signals for two feeds, $x(i)$ and $y(i)$ (where i indicates the time) will have the properties

$$E\left[x(i)x(j)\right] = \sigma_x^2 \delta_{ij}$$

$$E\left[y(i)y(j)\right] = \sigma_y^2 \delta_{ij}$$

$$E\left[x(i)y(j)\right] = \rho_{xy}\sigma_x\sigma_y\delta_{ij}$$

where $|\rho_{xy}| \leq 1$. Here we used the fact that samples of white noise taken at the Nyquist rate are uncorrelated. Writing the single-bit quantized samples as $\hat{x}(i) = \pm 1, \hat{y}(i) = \pm 1$, and assuming Gaussian noise processes, the correlation coefficient of the samples is [7]

$$\rho_{\hat{x}\hat{y}} = \langle \hat{x}(i)\hat{y}(i) \rangle = \frac{2}{\pi} \arcsin \rho_{xy} \simeq \frac{2}{\pi}\rho_{xy}$$

for $|\rho_{xy}| << 1$.

The Block II VLBI processor correlates each pair of signals, typically integrating for 2 s, producing sums for each pair:

$$u_{xy} = \frac{1}{N}\sum_{i=1}^{N} \hat{x}(i)\hat{y}(i)$$

where N is the number of samples integrated, which has the expectation value $E(u_{xy}) = \rho_{\hat{x}\hat{y}} \simeq (2/\pi)\rho_{xy}$ for $\rho_{xy} << 1$. The variance on a single product in the sum is

$$\sigma^2_{\hat{x}\hat{y}} = E\left[(\hat{x}\hat{y})^2\right] - \left[E\left(\hat{x}\hat{y}\right)\right]^2 = 1 - \rho^2_{\hat{x}\hat{y}} \simeq 1$$

The correlation sum is an average of such products, and each product is uncorrelated with any other, so the variance on the correlation sum is $\sigma^2_{u_{xy}} \simeq (1/N)$. Thus, the correlation coefficient of two signals can be obtained from the correlation sum by $\rho_{xy} \simeq (\pi/2)u_{xy}$ with uncertainty $\sigma_{\rho_{xy}} \simeq (\pi/2)(1/\sqrt{N})$.

There is one more complication: The elements of the noise correlation matrix described in this article are correlations among complex signals rather than the real ones described above, the complex signals being composed of the real signal plus its quadrature signal as the imaginary part. The correlation coefficients are likewise complex. Most of the above results still hold if you replace the products of the real signals by products of a complex signal and conjugated complex signal. A complex correlation sum is a combination of four real correlation sums:

$$u_{xy} = \frac{1}{N}\left(\sum_{i=1}^{N} \hat{x}_R(i)\hat{y}_R(i) + \sum_{i=1}^{N} \hat{x}_I(i)\hat{y}_I(i) + i\sum_{i=1}^{N} \hat{x}_I(i)\hat{y}_R(i) - i\sum_{i=1}^{N} \hat{x}_R(i)\hat{y}_I(i)\right)$$

The complex correlation coefficient is $\rho_{xy} \simeq (\pi/4)u_{xy}$, where the additional factor of 1/2 is necessary to keep ρ_{xx} normalized to 1. The uncertainty on both the real and imaginary parts of ρ_{xy} is $\sigma_{\rho_{xy}} \simeq (\pi/4)\sqrt{2/N}$, where the additional factor of $\sqrt{2}$ comes from the two real correlation sums contributing to both the real and imaginary parts. The uncertainty of the magnitude of the correlation coefficient is the same.

The Mark III data used in this article were integrated for 2-s intervals in the Block II VLBI processor and then, in subsequent processing, further integrated to yield integrations of about 20 s. At a sample rate of 4×10^6 samples/s, the uncertainty on the real and imaginary parts of the correlation coefficients is 1.2×10^{-4}.